RSC Advances

PAPER

View Article Online
View Journal | View Issue

Open Access Article. Published on 27 October 2025. Downloaded on 1/19/2026 9:22:09 PM.
This article is licensed under a Creative Commons Attribution-NonCommercial 3.0 Unported Licence.

Check for updates

Cite this: *RSC Adv.*, 2025, **15**, 40789

A novel DOPO-containing polymer derived from a main-chain benzoxazine: synthesis, characterization and its effect on thermal stability and flame retardancy of epoxy resin

Wei Zhang, Min Liu, Honghui Cheng, Jiafeng Di, Geng Huang and Hua Lai *

The application of reactive macromolecular flame retardants in polymers is gaining increasing attention. In this study, the polymer PBOZ-DOPO was readily synthesized *via* nucleophilic addition between 9,10-dihydro-9-oxa-10-phosphaphenanthrene-10-oxide (DOPO) and a main-chain benzoxazine polymer (PBOZ). It was utilized as both a co-curing agent and polymeric flame retardant for epoxy resin, yielding epoxy thermosets designated as P_n, where *n* represented the phosphorus content in the cured polymers (*n* wt%). While all epoxy thermosets retained good transparency, the addition of PBOZ-DOPO reduced thermal stability, as indicated by thermogravimetric analysis (TGA) and dynamic mechanical analysis (DMA). Fortunately, the macromolecular structure and the presence of active OH groups in PBOZ-DOPO helped alleviate the decline in glass transition temperature (T_g). When the phosphorus content was below 0.5 wt%, the T_g loss was less than 10 °C. PBOZ-DOPO imparted highly efficient flame retardancy to the epoxy resin. With a phosphorus content of only 0.3 wt%, the epoxy thermoset P3 achieved a limiting oxygen index (LOI) of 34.1% and met the vertical burning (UL-94) V-0 rating. Cone calorimetry tests demonstrated a progressive decrease in heat release rate (HRR), total heat release (THR), and total smoke production (TSP) from P0 to P5. Scanning electron microscopy (SEM) and Raman spectroscopy further revealed that the amount of graphitized carbon layers formed during combustion increased consistently from P0 to P5, supporting the enhanced flame-retardant performance. Tensile tests indicated that the incorporation of PBOZ-DOPO did not significantly compromise tensile strength or elongation at break, particularly in the case of P3. Overall, the results confirmed that PBOZ-DOPO was an excellent flame retardant with well-balanced properties for epoxy resin.

Received 12th September 2025
Accepted 20th October 2025

DOI: 10.1039/d5ra06895a

rsc.li/rsc-advances

Introduction

Epoxy resin is an important thermosetting polymer widely used in coatings, adhesives, resin matrix composites,[1] and more importantly, in circuit boards[2] among other applications. This broad utility stems from its excellent mechanical and thermal properties, including high tensile strength and modulus, low water absorption, good solvent resistance, and relatively low dielectric constant and loss. However, like other hydrocarbon-based polymers, epoxy resin is highly flammable and often fails to meet flame-retardancy requirements for practical use. Halogenated flame retardants, such as tetrabromobisphenol A, have traditionally been employed to enhance flame resistancy. Nevertheless, their application is increasingly restricted due to the release of corrosive and toxic gases during combustion.[3] In recent years, phosphorus-containing organic compounds have emerged as promising alternatives. Among them, 9,10-dihydro-9-oxa-10-phosphaphenanthrene −10-oxide (DOPO) has proven to be an effective phosphorus source.[4–6] It can be utilized to construct various flame-retardant structures through several reactions, including: the Atherton–Todd reaction with amines or alcohols,[7,8] addition reactions with double bonds in Schiff bases,[9] olefins,[10] aldehydes and ketones,[11,12] and ring-opening reactions with heterocycles such as epoxides[13] or benzoxazines.[14–16]

The nucleophilic addition of DOPO to heterocyclic benzoxazines, first reported by the Lin group,[14] proceeds homogeneously in THF at room temperature, producing bisphenols in over 90% yield with high purity without the need for further purification. Given that benzoxazines are widely synthesized from inexpensive amines, phenols, and formalin,[17,18] this reaction offers a versatile pathway for generating numerous DOPO-benzoxazine derivatives. When employed as flame retardants in epoxy resins, the hydroxyl (OH) groups in these derivatives enhance their solubility, facilitating the formation of transparent thermosets.[19] Furthermore, the OH groups can react with epoxy groups, mitigating the migration of flame-retardant molecules from the matrix.[20,21] Additionally, the intramolecular synergy between

College of Chemistry and Material Science, Hengyang Normal University, Hengyang 421008, China. E-mail: laixhua163@163.com

© 2025 The Author(s). Published by the Royal Society of Chemistry

Open Access Article. Published on 27 October 2025. Downloaded on 1/19/2026 9:22:09 PM. This article is licensed under a Creative Commons Attribution-NonCommercial 3.0 Unported Licence.

phosphorus and nitrogen in these molecules further enhances flame retardancy.[22–24] In subsequent work, Lin *et al.* incorporated such bisphenols as flame retardants in epoxy resin and achieved a UL-94 V-0 rating with a phosphorus content as low as 1.22 wt%.[16] Similarly, Wang *et al.* synthesized a phosphorus/nitrogen-containing compound (DOPO-BAPh) bearing a phthalonitrile-functionalized benzoxazine. With only 0.26 wt% phosphorus content, the modified epoxy thermosets exhibited a limiting oxygen index (LOI) of 35.8% and achieved a V-0 rating in UL-94 testing.[15]

However, the introduction of organic flame retardants usually deteriorated thermal properties of epoxy thermosets, especially for glass transition temperature (T_g).[16,25] In Lin's study, the T_gs of epoxy thermosets dropped sharply (more than 40 °C) when the phosphorus flame retardant was introduced (0.78 wt%).[16] In order to maintain high T_g of epoxy thermosets, oligmeric or macromolecular flame retardants were developed in recent studies.[26,27] Wang synthesized a DOPO-based oligomer named PDAP *via* the nucleophilic addition reaction between DOPO and imine.[28] A slight decrease less than 10 °C in T_g was observed with the incorporation of PDAP into epoxy thermosets, from 171 °C of pure epoxy thermoset to 163 °C of epoxy thermosets with 7 wt% of PDAP. Chen observed only 8 °C loss of T_g caused by adding 15 wt% flame retardant poly(piperazine phosphaphenanthrene) (DOPMPA).[29] Luo reported a hyperbranched polyamide oligomer containing DOPO (HPD).[30] All the epoxy resin samples containing HPD had slightly higher T_g than pure epoxy thermoset, which might be related with increased cross-linking density owing to HPD's hyperbranched polymeric structure.

To address the demand for comprehensive performance in flame-retarded epoxy resins, a novel polymeric flame retardant, PBOZ-DOPO, was designed and synthesized. The synthesis involved a straightforward two-step procedure: a Mannich-type polymerization followed by an addition reaction, using bisphenol A (BPA), 4,4′-diaminodiphenylmethane (DDM), paraformaldehyde (PF) and DOPO as raw materials. This strategy offered advantages such as low cost, mild reaction conditions, and high yield. The resulting PBOZ-DOPO, featuring both macromolecular structure and active hydroxyl groups, was incorporated into epoxy resin as a co-curing agent and flame retardant. This macromolecular design of PBOZ-DOPO would promote excellent dispersion of PBOZ-DOPO within the epoxy matrix, leading to comprehensive performances including transparency, thermal stability, and flame retardancy of the epoxy thermosets. The effects of PBOZ-DOPO on the thermal, mechanical, and flame-retardant properties of the epoxy thermosets were then systematically investigated using TGA, DMA, tensile tests, LOI and UL-94 tests, and cone calorimetry. Furthermore, the flame-retardant mechanism was elucidated by analyzing residual chars and pyrolytic gases *via* SEM, Raman spectroscopy, and thermogravimetric analysis-infrared spectrometry (T_g-IR).

Experimental

Materials

DDM and BPA were purchased from Aladdin reagent Co., Ltd and recrystallized by toluene. DOPO, paraformaldehyde (PF), $CHCl_3$, triethanolamine (TEOA) and *N*,*N*-dimethylformamide (DMF) were AR grade and purchased form Sinopharm Chemical Reagent Co., Ltd. Epoxy resin (E51) with an epoxy value of 0.51 mol/100 g was supplied by Epoxy Resin Division of Baling Petrochemical Co., Ltd.

Synthesis of PBOZ

BPA (11.2 g, 0.05 mol), DDM (9.9 g, 0.05 mol), PF (7.2 g, 0.24 mol) were added into a three-necked flask equipped with a nitrogen inlet and condenser, followed by introduction of $CHCl_3$ (60 mL) and TEOA (15 mL). The reaction mixture was stirred at 80 °C for 24 h. The solution obtained was then dropped into methanol. The precipitate was filtered and washed with deionized water. After drying at 105 °C in a vacuum oven, white powder (25.6 g, 97.0%) was obtained.

Preparation of PBOZ-DOPO

PBOZ (20.0 g, 0.042 mol calculated by repeating unit) and DOPO (19.1 g, 0.088 mol) were dissolved in DMF (60 mL) and stirred at room temperature for 24 h. The solution was dropped into a beaker filled with distilled water, and white flakes were precipitated, filtered and washed with distilled water. The resulting solid was placed in a vacuum oven at 90 °C to obtain a light green solid (36.1 g, 92.3%).

Preparation of epoxy thermosets P0–P5

The curing agent DDM and the flame retardant PBOZ-DOPO are mixed and heated to 120 °C to obtain a homogeneous melt. After the melt was cooled to 90 °C, it was quickly poured into epoxy resin (E51) of 70 °C and stirred heavily to obtain transparent glue. The glue was poured into silicone molds, placed in a vacuum oven for 10 minutes to remove air bubbles, and then cured at 130 °C for 2 h followed by 170 °C for a further 2 h. The mass ratio of E51/DDM/PBOZ-DOPO was listed in Table 1 with calculated phosphorus contents according to the reaction formulation.

Characterization

^{1}H nuclear magnetic resonance (^{1}H NMR, 500 MHz) and ^{31}P nuclear magnetic resonance (^{31}P NMR, 202 MHz) spectra were recorded on Bruker Avance III HD spectrometer using $CDCl_3$ or DMSO-d_6 as solvents. Fourier transform infrared (FTIR) spectra of the samples were measured on an IRPrestige-21 instrument (Shimadzu, Japan) by the transmission method using the KBr pellet technique. Gel permeation chromatography (GPC) was performed by Waters 515 in DMF, using polystyrene standards for calibration. Ultraviolet-Visible (UV) spectra of epoxy thermosets with a thickness of 2 mm were analyzed by Ultraviolet-Visible Spectrophotometer (Shimadzu UV-2450) and the detection wavelength varied between 350 and 800 nm. TGA was conducted using a STA 449 F3 thermal analyzer (NETZSCH, Germany) under air gas flow of 50 mL min^{-1}. The samples (about 7 mg) were heated from room temperature to 800 °C at a linear heating rate of 10 °C min^{-1}. TG-IR involved utilizing a Q5000 thermogravimetric analyzer (TA) in conjunction with

 © 2025 The Author(s). Published by the Royal Society of Chemistry

Open Access Article. Published on 27 October 2025. Downloaded on 1/19/2026 9:22:09 PM. This article is licensed under a Creative Commons Attribution-NonCommercial 3.0 Unported Licence.

Table 1 Formulations of epoxy thermosets cured with various amount of PBOZ-DOPO

Sample	E51 (g)	DDM (g)	PBOZ-DOPO (g)	PBOZ-DOPO content (wt%)	P content (wt%)
P0	100.00	26.77	0.00	0.0	0.0
P1	100.00	26.57	1.82	1.4	0.1
P2	100.00	26.37	3.69	2.8	0.2
P3	100.00	26.16	5.60	4.3	0.3
P4	100.00	25.94	7.57	5.7	0.4
P5	100.00	25.72	9.59	7.0	0.5

an IS20 FT-IR spectrophotometer (Thermo Fisher Scientific). The analysis was conducted in a nitrogen atmosphere, with a temperature range of 30 °C to 800 °C while heating at a rate of 10 °C min^{-1}. DMA were measured with a DMA Q800 (TA, USA). The dynamic storage modulus was determined at a frequency of 1 Hz and a heating rate of 5 °C min^{-1} over the range of 25 °C to 250 °C. The dimensions of the samples were approximately 50 × 10 × 5 mm. SEM images were gained by a Zeiss EVO 10 at 20 kV. UL-94 tests were conducted by a CZF-II horizontal and vertical burning tester (Jiangning Analysis Instrument Co., China) according to ASTM D3801. The dimensions of the samples were 127 × 12.7 × 3 mm. LOI was measured by an HC-2 oxygen index meter 207 (Jiangning Analysis Instrument Co., China) according to ASTMD 2863. The dimensions of each specimen were 100 × 6.5 × 3 mm. Combustion and charring behaviors were studied using a Testech cone calorimeter according to ISO 5660 at an external heat flux of 35 kW m^{-2}. The dimension of specimen was 100 × 100 × 3 mm. X-ray diffraction (XRD) was performed on a Shimadzu XRD-6100 X-ray diffraction spectrometer with a Cu-Kα radiation source in the 2θ range of 5–80°, with a scanning speed of 0.6° per s. The laser Raman spectroscopy measurement was conducted at room temperature using a XRD01 Raman apparatus (Thermo Fisher Scientific), with an excitation wavelength of 633 nm and a scanning range of 100–3500 cm^{-1}. Tensile properties were measured using an electronic universal testing machine (CMT-10, Liangong, China) with a crosshead speed of 10 mm min^{-1} at room temperature, following GBT 1040.1-2006.

Results and discussion

Synthesis and characterization of PBOZ-DOPO

The flame retardant PBOZ-DOPO was synthesized through two-step reactions, as shown in Scheme 1. Firstly, polymeric PBOZ, a main-chain benzoxazine, was prepared through Mannich-type polycondensation with DDM, BPA and PF. When the reaction was carried out in a mixed solvent of toluene/ethanol, PBOZ had a small number molecular weight (M_n) of 4200.[31] The use of $CHCl_3$/TEOA (v/v = 4 : 1) as solvent could raise M_n of PBOZ up to 10 000 with a good yield of 97.0%.[32] Then, PBOZ-DOPO was prepared by addition reaction between PBOZ and DOPO. Instead of using THF as the solvent reported in the literature,[14] DMF was chosen in order to improve the solubility of the starting materials. Since oxazine ring may open at high temperature to form undissolved gel, the reaction should be carried out at room temperature. The yield of PBOZ-DOPO was up to 92.3%. Owing to the low-cost starting materials, straightforward reaction process, and high yield, PBOZ-DOPO can be readily prepared on a kilogram scale, indicating its high commercial potential.

The GPC curves of PBOZ and PBOZ-DOPO were shown in Fig. 1a. PBOZ-DOPO had a M_n of about 8500 g mol^{-1}, slightly lower than that of PBOZ. This might be attributed to PBOZ's rigid and cyclic main-chain structure, resulting in a larger hydrodynamic volume than that of PBOZ-DOPO,[27] even though the latter had extra rigid DOPO groups. FTIR spectra of DOPO, PBOZ and PBOZ-DOPO were displayed in Fig. 1b. There were characteristic peaks at 2434 cm^{-1} ascribed to P–H in the spectrum of DOPO and at 943 cm^{-1} ascribed to oxazine ring in the spectrum of PBOZ. These peaks disappeared in the spectrum of PBOZ-DOPO. Fig. 1c showed the ^{1}H NMR spectra of DOPO, PBOZ and PBOZ-DOPO. As to DOPO, the peak at 8.74 ppm was assigned to the proton in P–H. For PBOZ, there were two obvious peaks near 4.54 ppm and 5.30 ppm attributed to methylene proton on oxazine ring. Compared with DOPO and PBOZ, the above-mentioned peaks at 8.74 ppm, 4.54 ppm and 5.30 ppm were not observed in the spectrum of PBOZ-DOPO, but a new peak at 4.1 ppm corresponding to proton on *N*–

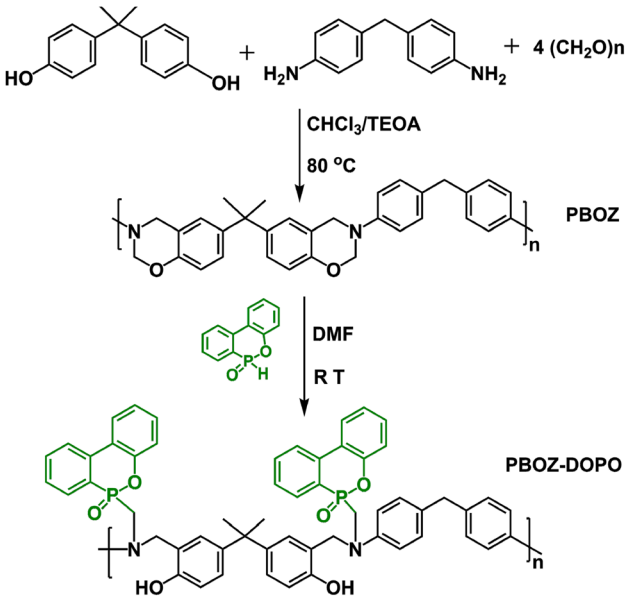

Scheme 1 Synthetic route of PBOZ-DOPO.

Open Access Article. Published on 27 October 2025. Downloaded on 1/19/2026 9:22:09 PM.
This article is licensed under a Creative Commons Attribution-NonCommercial 3.0 Unported Licence.

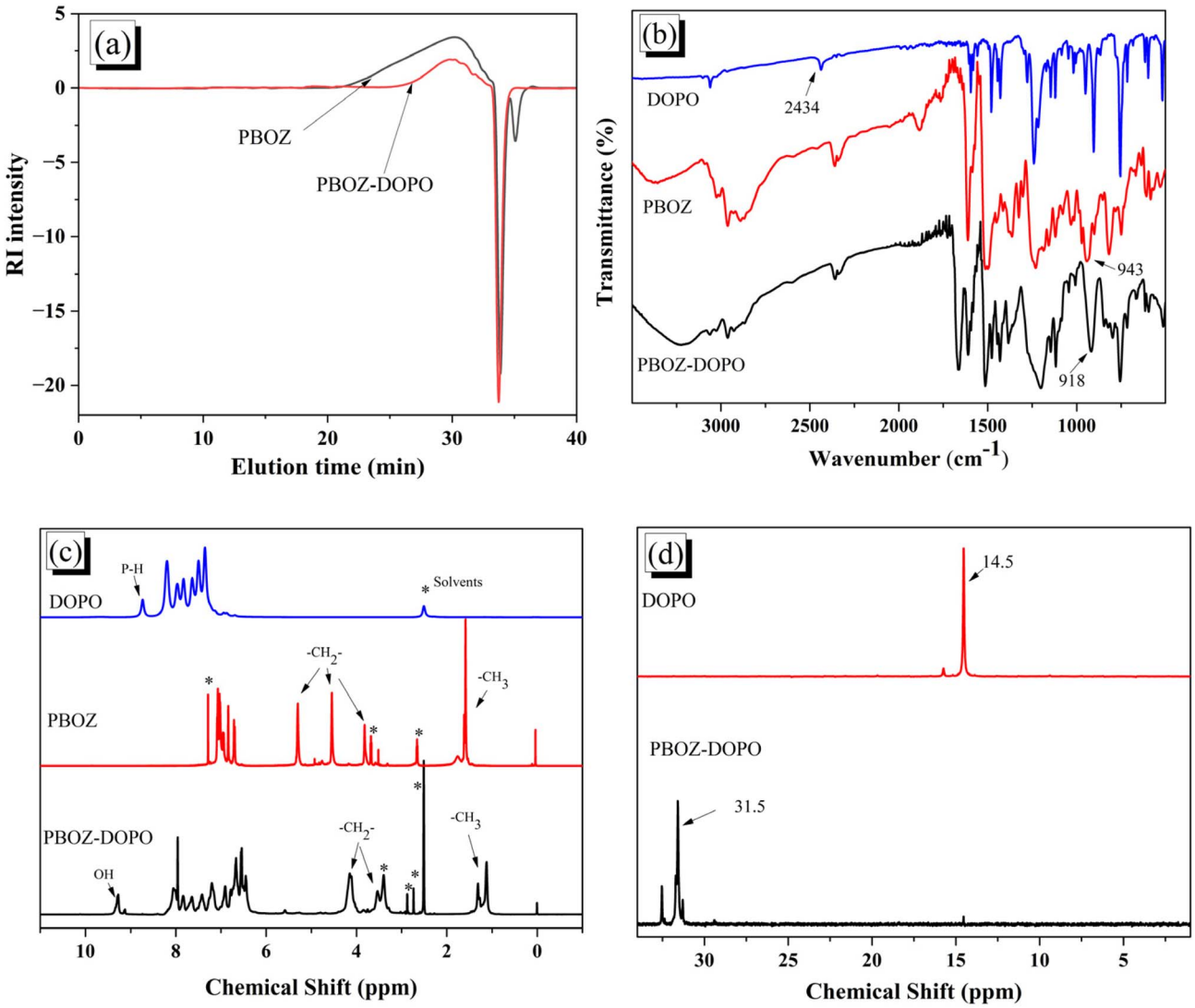

Fig. 1 (a) GPC trace, (b) FTIR, (c) ^{1}H NMR and (d) ^{31}P NMR spectra of DOPO, PBOZ and PBOZ-DOPO.

CH_2–P appeared. In the ^{31}P NMR spectrum of BOZ-DOPO showed in Fig. 1d, a main peak appeared at 31.58 ppm, while the 14.5 ppm peak ascribed to DOPO was almost not seen.

For further certify the structure of PBOZ and PBOZ-DOPO, comparative characterizations were carried out for a small benzoxazine BOZ and it's derivative BOZ-DOPO shown in Fig. 2a. It was found that no obvious change of in the FTIR (Fig. 2b) and NMR (Fig. 2c and d) spectra between BOZ and PBOZ or between BOZ-DOPO and PBOZ-DOPO. Therefore, it could be concluded that PBOZ-DOPO with the molecular structure shown in Scheme 1 was synthesized successfully.

Transparency of epoxy thermosets

Due to the poor compatibility, commonly flame retardants, like ammonium polyphosphate (APP), $Al(OH)_3$, melamine and some organic heterocyclic compounds, were hardly be dissolved in epoxy at molecular level. This significantly reduced the transparency of the resulting products. Similarly, most polymers reported were less soluble in epoxy resin compared with small organic molecules, which greatly affected the transparency. Fortunately, PBOZ-DOPO was found soluble in DDM at a high temperature of 120 °C, which allowed the three components, E51/DDM/PBOZ-DOPO, to form a transparent viscous solution when mixed at 70 °C. After cured at high temperature, epoxy thermosets possessed good transparency even at the highest dosage of 7.0 wt% of PBOZ-DOPO, which can be seen in Fig. 3. Good solubility of PBOZ-DOPO in DDM and epoxy resin was resulted from its' linear molecular structure and the presence of many OH groups which could be chemically bonded on epoxy molecules, as illustrated in Fig. 4a. Such compatibility between the flame retardant and matrix was considered beneficial for transparency, thermal and mechanical properties. Fig. 4b showed UV spectra of epoxy thermosets with a thickness of 2 mm. Compared with P0, the incorporation of the flame retardant induced a red-shift in the transmittance curves of P1, P3 and P5, which became more pronounced with increasing flame

 © 2025 The Author(s). Published by the Royal Society of Chemistry

Open Access Article. Published on 27 October 2025. Downloaded on 1/19/2026 9:22:09 PM.
This article is licensed under a Creative Commons Attribution-NonCommercial 3.0 Unported Licence.

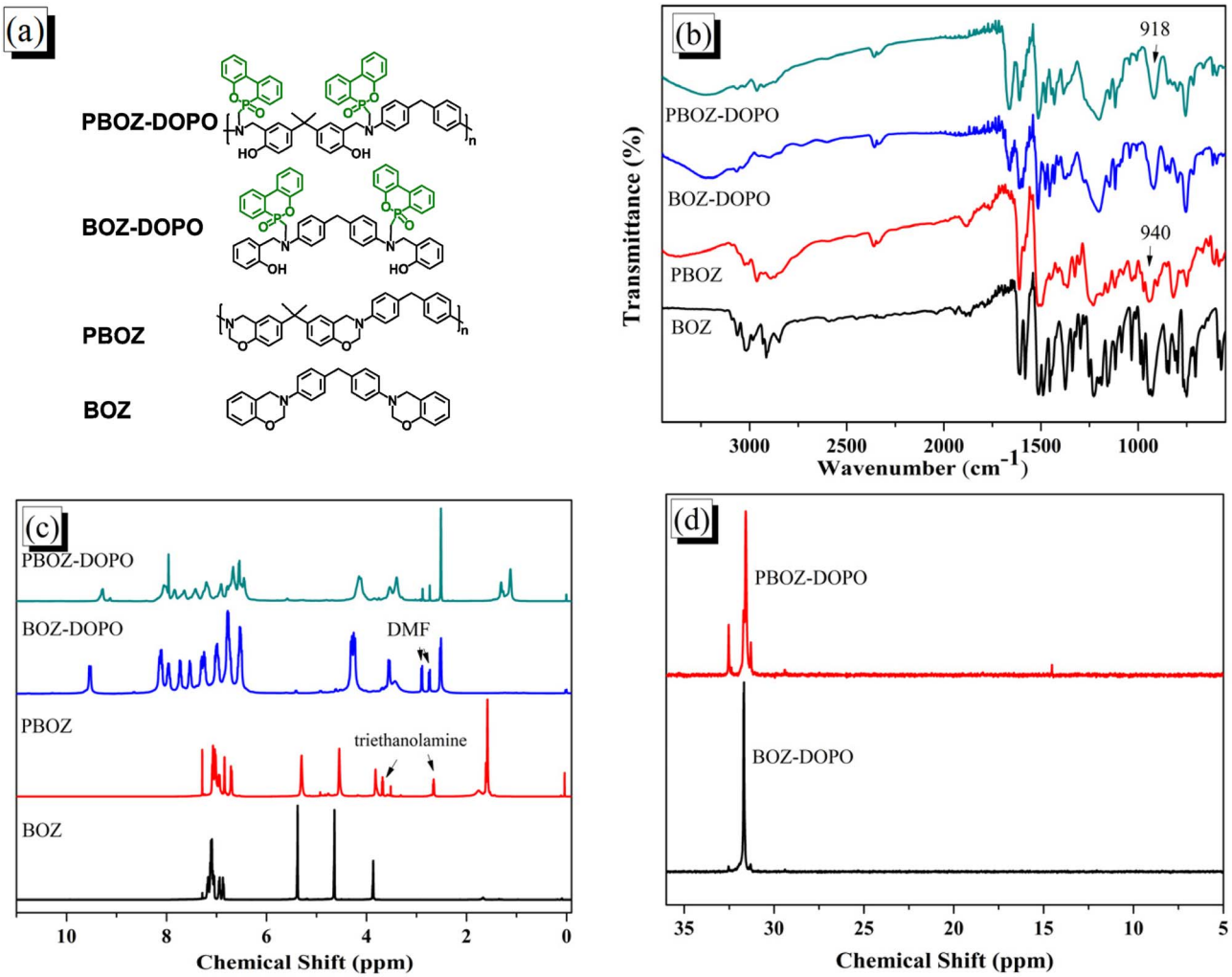

Fig. 2 (a) Molecular structures, (b) FTIR, (c) ^{1}H NMR and (d) ^{31}P NMR spectra of BOZ, PBOZ, BOZ-DOPO and PBOZ-DOPO.

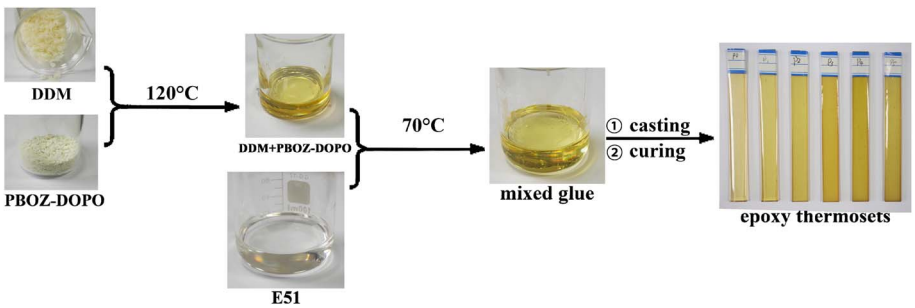

Fig. 3 Preparation route and optical images of epoxy thermosets.

retardant loading. As a result, P1, P3, and P5 exhibited progressively deeper yellow coloration (Fig. 3). This phenomenon was attributed to the conjugated structure of DOPO in PBOZ-DOPO that could absorb certain light with wavelength near 400 nm. However, beyond 500 nm wavelength, the addition of the flame retardant helped maintain or even enhance the transmittance, thereby ensuring that all cured epoxy resins retained satisfactory transparency.

Thermal stability of thermosets

The effect of introduction of PBOZ-DOPO on the thermal properties of epoxy thermosets was measured by TGA. The results were shown in Fig. 5 and the corresponding data was listed in Table 2. The neat epoxy themoset P0 exhibited a temperature at 5% weight loss ($T_{5\%}$) of 376.9 °C. With the addition of PBOZ-DOPO, the $T_{5\%}$ of epoxy themosets P1–P5 all declined. P2 with 0.2 wt% phosphorous content had the lowest

Open Access Article. Published on 27 October 2025. Downloaded on 1/19/2026 9:22:09 PM.
This article is licensed under a Creative Commons Attribution-NonCommercial 3.0 Unported Licence.

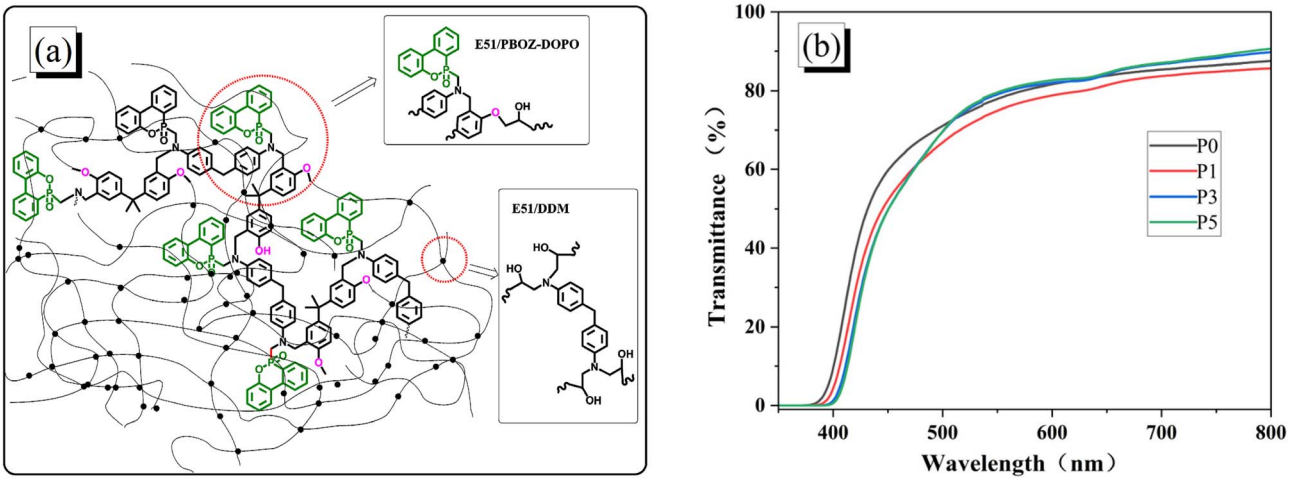

Fig. 4 (a) Proposed structure and (b) UV spectra of epoxy thermosets.

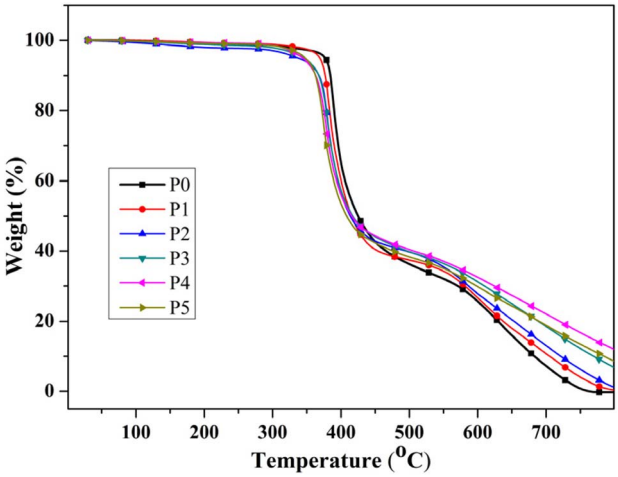

Fig. 5 TGA curves of epoxy thermosets in air.

$T_{5\%}$ of 337 °C, while P3, P4 and P5 with phosphorous content 0.3–0.5 wt% showed $T_{5\%}$ above 340 °C. The degradation of thermal stability caused by introduction of PBOZ-DOPO was resulted from weak bond P–O in PBOZ-DOPO. Nevertheless, the residue weight at 800 °C of P1–P5 were all higher than that of P0. The phosphorous acid produced from earlier combustion of PBOZ-DOPO could promote the carbonization of epoxy matrix. The residual weight reached a maximum of 11.80 wt% for P4 with 0.4 wt% phosphorus content. With regard to P5 with 0.5 wt% phosphorous content, the residue weight had some decline compared with that for P4, which might be resulted from sharp decrease of cross-link density V_e as shown in Table 2.[33] However, all samples doping with PBOZ-DOPO showed a $T_{5\%}$ higher than 337 °C, indicating they could maintain good thermal stability compared with P0.

To investigate the effect of PBOZ-DOPO on the mechanical properties of epoxy thermosets, the DMA tests were performed, and the results were shown in Fig. 6. The storage modulus (E') at 30 °C of P0 was 1521 MPa. Generally, E' would drop when flame retardants were added in epoxy thermosets because of low cross-linking density. On the contrary, P1 and P2 gave increased E', 1743 MPa and 2141 MPa at 30 °C, indicating the introduction of PBOZ-DOPO was beneficial for enhancing stiffness of epoxy thermosets. However, further increasing PBOZ-DOPO led to sharp decline of E'. The values of E' of P3, P4 and P5 were 1930 MPa, 1445 MPa and 1428 MPa, respectively. This might be attributed to the significant influence of PBOZ-DOPO on the crosslinking density when its content exceeded 2.8 wt%.

From the curves of the loss factor (tan δ) *versus* temperature in Fig. 6b, T_gs of samples P0–P5 were recorded and listed in Table 2. P0 displayed the highest T_g of 172.9 °C. With the PBOZ-

Table 2 TGA and DMA data for epoxy thermosets

Sample	P content (wt%)	$T_{5\%}$ (°C)	Residual weight at 800 °C (wt%)	E' at 30 °C (MPa)	V_e[a] (10^{-3} mol m^{-3})	T_g (°C)
P0	0.0	376.9	0.00	1521	2.34	172.9
P1	0.1	368.9	0.36	1743	2.10	166.4
P2	0.2	337.2	1.06	2141	1.86	167.5
P3	0.3	346.7	6.74	1930	1.91	163.8
P4	0.4	343.9	11.80	1445	1.70	163.7
P5	0.5	348.0	8.51	1428	1.17	141.1

[a] V_e = the storage modulus (E') at T_g + 30 °C/3R(T_g + 30), where R represents the ideal gas constant.

 © 2025 The Author(s). Published by the Royal Society of Chemistry

Open Access Article. Published on 27 October 2025. Downloaded on 1/19/2026 9:22:09 PM.
This article is licensed under a Creative Commons Attribution-NonCommercial 3.0 Unported Licence.

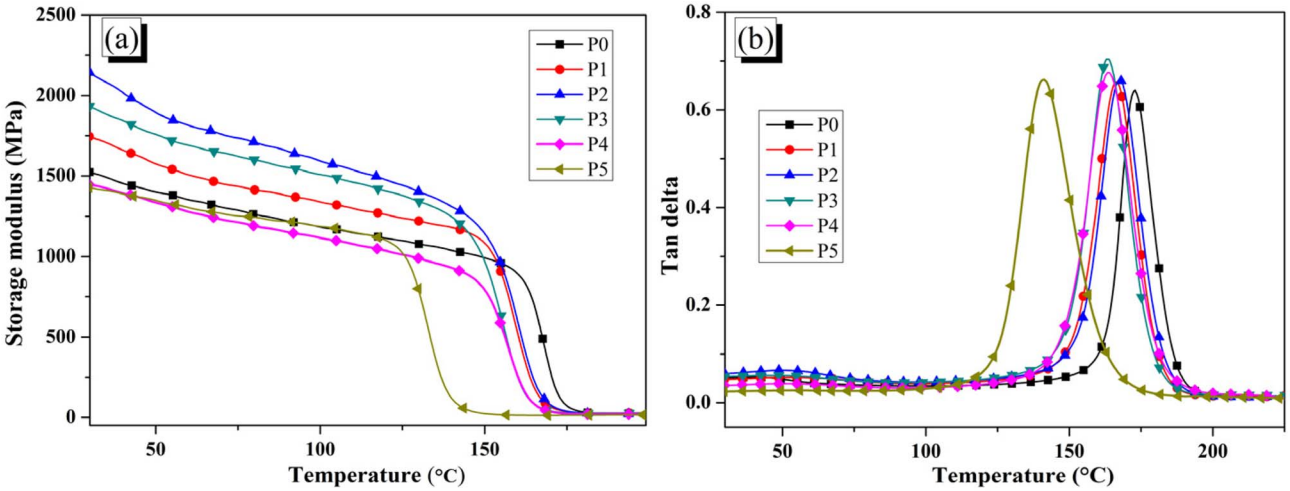

Fig. 6 (a) E' and (b) tan δ *versus* temperature curves of epoxy thermosets.

DOPO content increased gradually from 0 wt% to 7.0 wt% for P0 to P5, T_gs exhibited a decreasing trend. There was a rapid decline of T_g for P5 due to severe damage of cross-linking structure by addition of 7.0 wt% PBOZ-DOPO, which was consistent with the TGA data. However, it was worth noting that only less than 10 °C of loss in T_g were observed for P1–P4. The macromolecular structure and lots of active phenol OH groups in PBOZ-DOPO were speculated to be accounted for the maintenance of T_g values. As illustrated in Fig. 4a, PBOZ-DOPO was chemically linked with epoxy molecules through –O– bond. Therefore, the cross-linking density was remained to a large extent.

Flame retardancy of epoxy thermosets

The flame retardancy of epoxy thermosets was evaluated by UL-94 and LOI tests. As shown in Table 3, the sample P0 obtained from E51/DDM without any flame retardant had a low LOI of 25.7%. When 1.4 wt% PBOZ-DOPO was introduced, the LOI value of P1 was elevated to 30.4%. With further increasing the content of PBOZ-DOPO, the LOI values of the corresponding samples continuously were enhanced. The highest LOI value reached up to 36.1% for P5 with 7.09 wt% content of PBOZ-DOPO in the epoxy thermoset. In terms of UL-94 tests, epoxy thermosets P0 and P1 had no UL-94 rating, while sample P2 with 2.8 wt% PBOZ-DOPO passed V-1 rating. As the PBOZ-DOPO content was equal to or larger than 4.3 wt%, the samples could all achieve V-0 rating. It was worth noting that 4.3 wt% PBOZ-DOPO content corresponded to a relatively low phosphorous content of 0.3 wt%, demonstrating that PBOZ-DOPO was a high-efficient flame retardant for epoxy resin. The good result was suggested to be attributed to intramolecular P–N synergistic effect formed by the P provided by DOPO and the N in PBOZ-DOPO, which was often seen in P, *N*-containing flame retardants derived from DOPO and Schiff bases.[9,34]

Cone calorimetry was employed to evaluate the combustion behavior of the epoxy thermosets. Fig. 7 presents the heat release rate (HRR), total heat release (THR), and total smoke production (TSP) for samples P0, P1, P3, and P5. As shown in the HRR curves (Fig. 7a), the time to ignition (TTI) of the neat epoxy (P0) was 100 s. The incorporation of PBOZ-DOPO reduced the TTI, a phenomenon consistent with previous reports on phosphorus-containing flame retardants.[15,25] Interestingly, the TTI values decreased only slightly as the PBOZ-DOPO content increased from 1.4 wt% to 7.0 wt%. After ignition, the pristine epoxy (P0) exhibited a high peak heat release rate (PHRR) of 800 kW m^{-2}. In contrast, the PHRR gradually decreased with increasing PBOZ-DOPO loading, dropping to 675 kW m^{-2} for P1 and further to 470 kW m^{-2} for P5. A similar trend was observed for the THR (Fig. 7b), which declined continuously from 81 MJ m^{-2} for P0 to 37 MJ m^{-2} for P5. Moreover, the TSP values of the

Table 3 Flammability test results of epoxy thermosets

				UL-94		
Sample	PBOZ-DOPO content (wt%)	P content (wt%)	LOI (%)	$t_1 + t_2$ (s)	Dropping	Rating
P0	0.0	0.0	25.7	44.2 + 94.5	YES	No
P1	1.4	0.1	30.4	14.6 + 81.1	NO	No
P2	2.8	0.2	31.8	6.7 + 4.3	NO	V-1
P3	4.3	0.3	34.1	6.0 + 3.0	NO	V-0
P4	5.7	0.4	35.8	2.4 + 1.2	NO	V-0
P5	7.0	0.5	36.1	1.1 + 0.8	NO	V-0

Open Access Article. Published on 27 October 2025. Downloaded on 1/19/2026 9:22:09 PM.
This article is licensed under a Creative Commons Attribution-NonCommercial 3.0 Unported Licence.

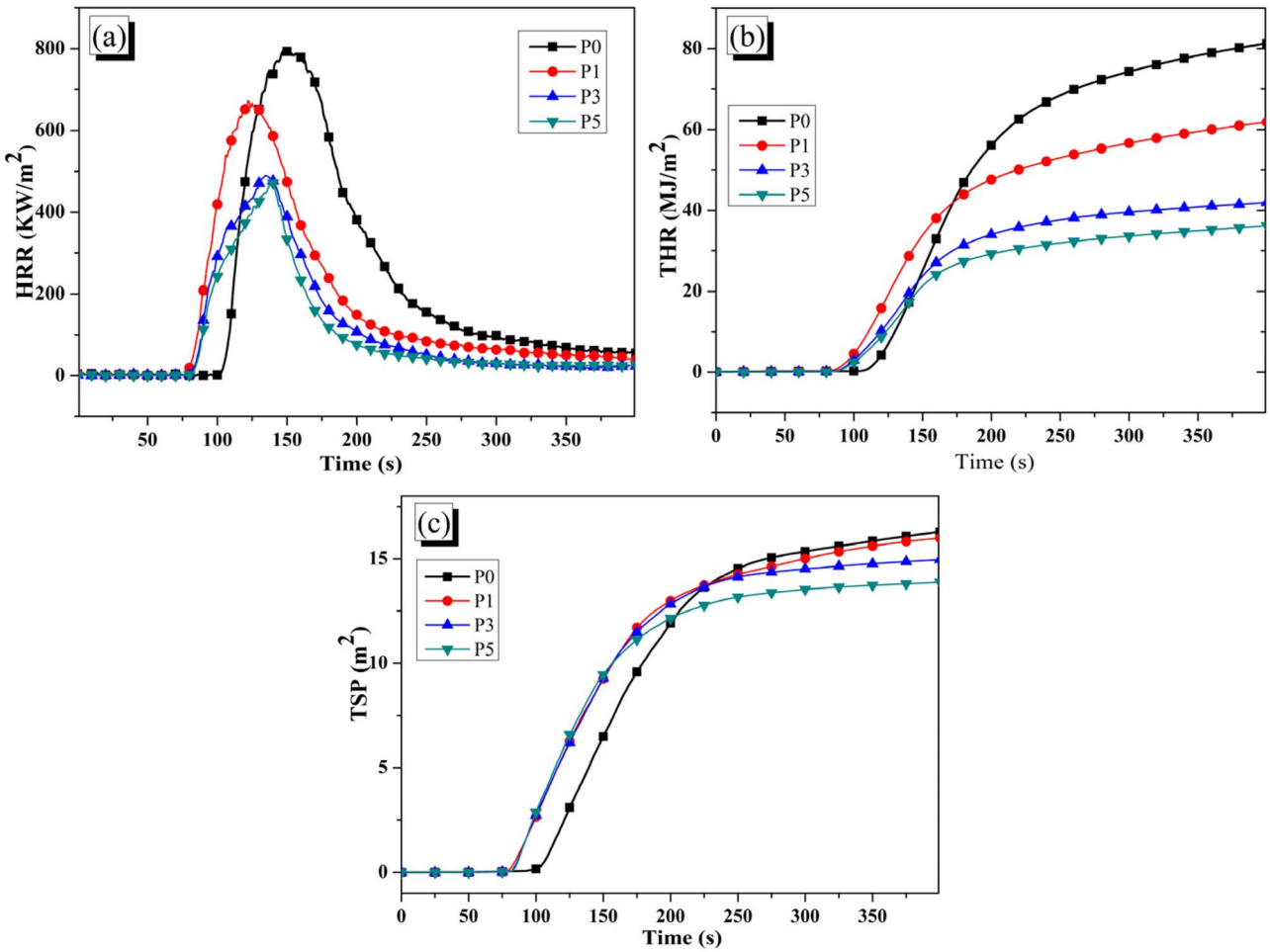

Fig. 7 Cone calorimetric curves of epoxy thermosets: (a) HRR; (b) THR; (c) TSP.

flame-retardant samples were notably lower than that of P0 (Fig. 7c), indicating that PBOZ-DOPO also contributed to smoke suppression. Visual inspection of the residues after testing (Fig. 8a) revealed a marked difference in char height: less than 1 cm for P0, but greater than 2 cm for P1–P5, with the height increasing monotonically with phosphorus content. The

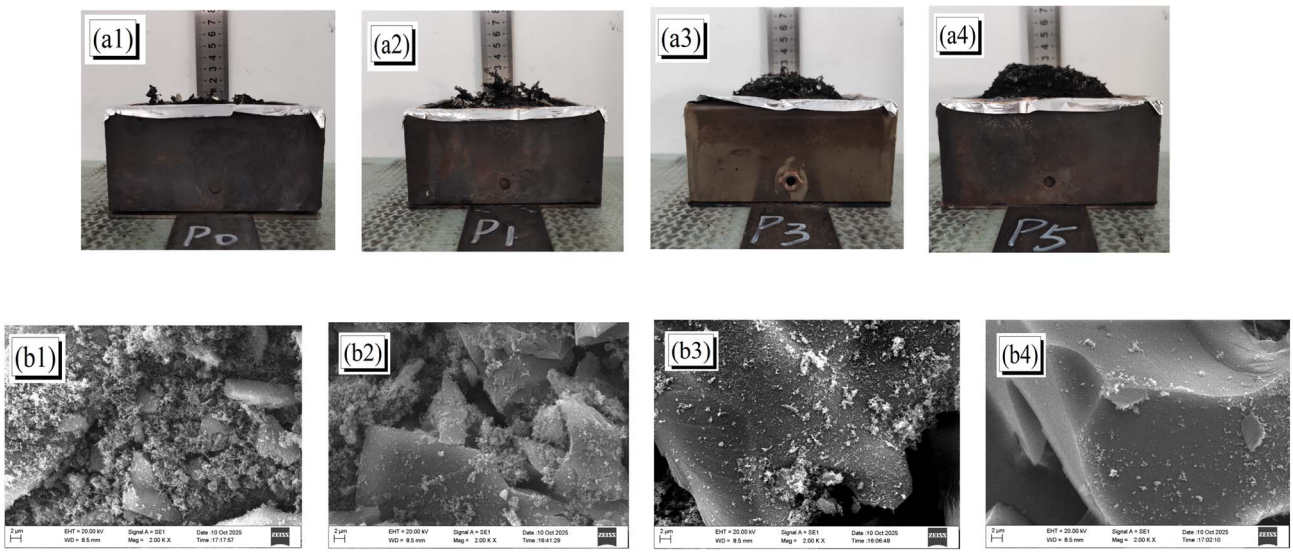

Fig. 8 (a) Optical images (a1–a4) and (b) SEM images (b1–b4) of residual chars from combustion of P0, P1, P3, and P5.

 © 2025 The Author(s). Published by the Royal Society of Chemistry

Open Access Article. Published on 27 October 2025. Downloaded on 1/19/2026 9:22:09 PM.
This article is licensed under a Creative Commons Attribution-NonCommercial 3.0 Unported Licence.

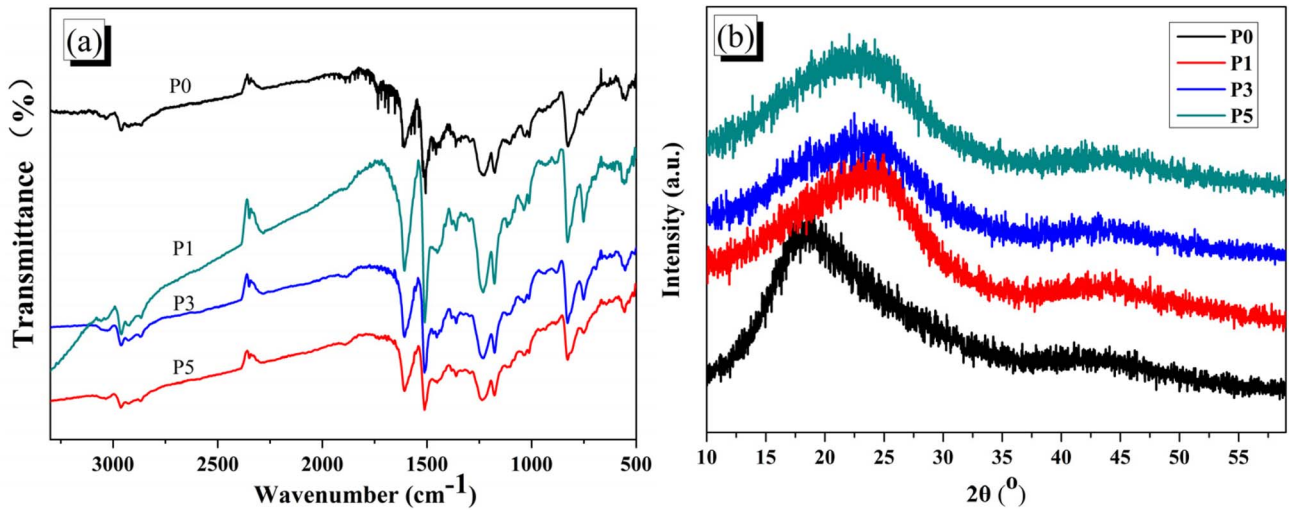

Fig. 9 (a) FTIR and (b) XRD patterns of residual chars.

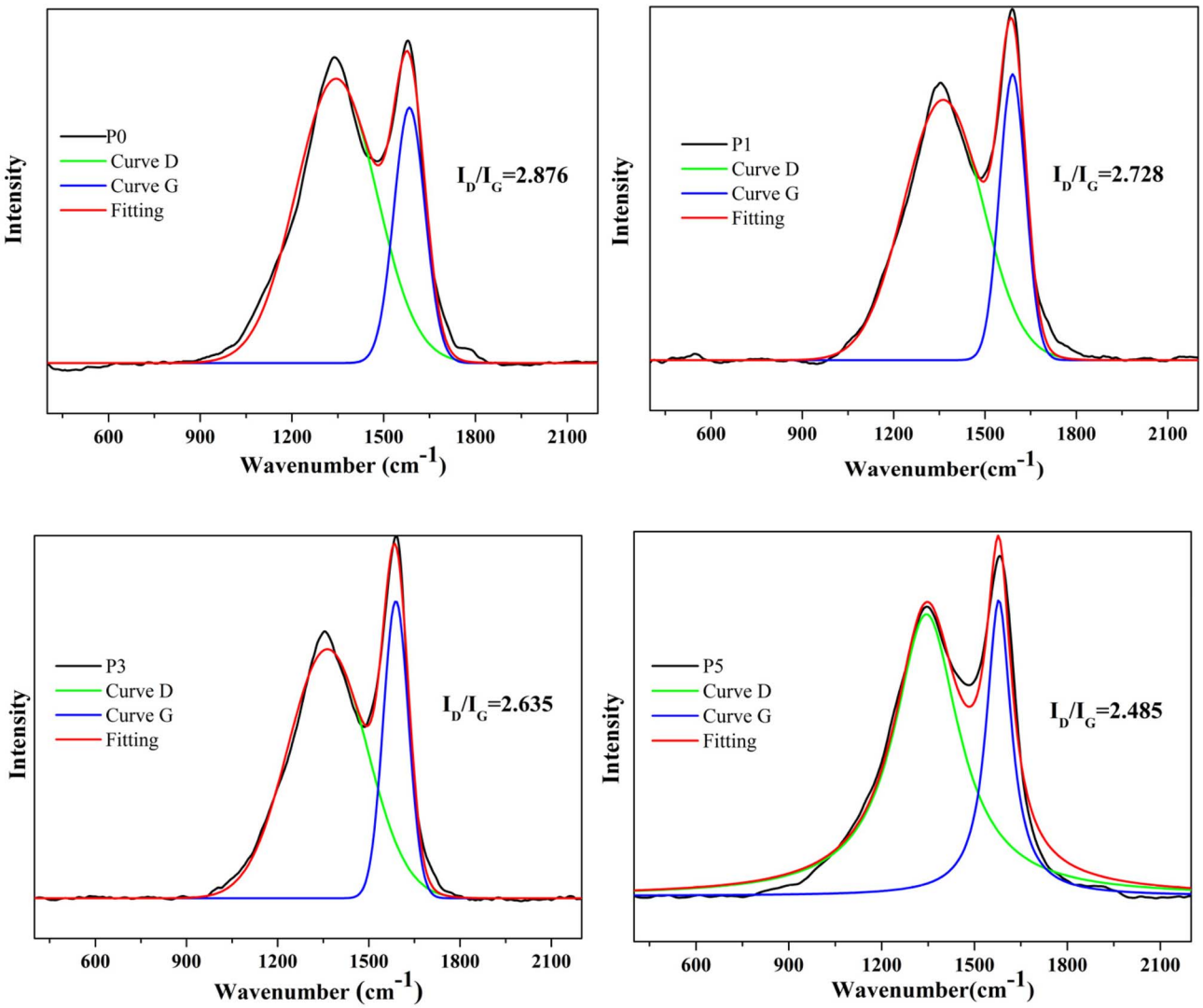

Fig. 10 Raman spectra of residual chars.

Open Access Article. Published on 27 October 2025. Downloaded on 1/19/2026 9:22:09 PM.
This article is licensed under a Creative Commons Attribution-NonCommercial 3.0 Unported Licence.

decrease of HRR, THR, and TSP and the increase of char height could be attributed to the increased production of phosphoric acid at higher dosages of PBOZ-DOPO, which promoted the carbonization of the epoxy resin.

Char analysis

To elucidate the flame-retardant mechanism, the residual chars of the epoxy composites after combustion were analyzed by FTIR and X-ray diffraction (XRD). As shown in Fig. 9a, the FTIR spectra of the chars from P0, P1, P3, and P5 showed no significant differences in their absorption peaks, which was attributed to the low phosphorus content in the formulations of all the epoxy thermosets. The XRD patterns in Fig. 9b further confirmed that all residual chars were amorphous, as indicated by the absence of sharp crystalline peaks. However, a notable shift of the broad diffraction peaks to higher 2θ values was observed for the chars containing PBOZ-DOPO (P1, P3, P5) compared to that of neat epoxy (P0). This observation, correlated with the progressively denser morphology of the residual chars obtained from P0 to P5 as revealed by SEM (Fig. 8b), indicates that the incorporation of PBOZ-DOPO facilitated graphitization of the epoxy resin during combustion.

The graphitization of residual chars was further investigated by Raman spectroscopy (Fig. 10). The Raman spectra of four chars show a similar typical feature of amorphous carbons: the disorder-induced D peak at about 1360 cm^{-1} and G peak at about 1600 cm^{-1}. The integral intensity ratio of D band to G band (I_D/I_G) is represented for the graphitized degree of the carbon materials.[35] The residual chars from P0, P1, P3, and P5 show a decrease trend in I_D/I_G: 2.876, 2.728, 2.635, and 2.485. This indicated that with the increase of PBOZ-DOPO, the graphitized carbon layer formed during combustion of epoxy resins increased continuously, which gave rise to an enhancing flame retardancy.

Analysis of pyrolytic gases

TG-IR analysis was conducted to investigate the gas-phase flame inhibition behavior of the epoxy thermosets. As shown in the 3D plots (Fig. 11a and b), both P5 and P0 released a considerable amount of volatile products around 400 °C. However, P5

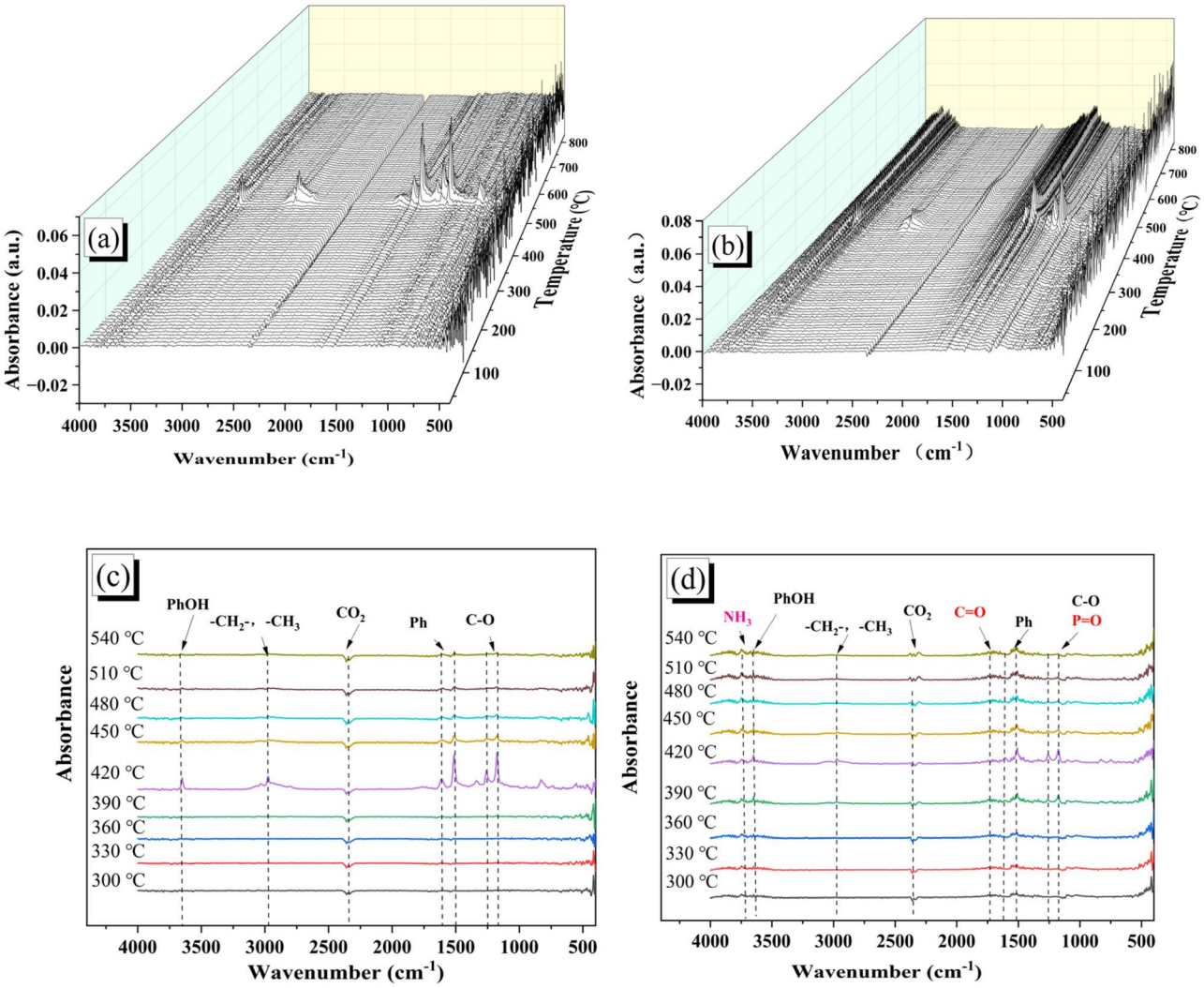

Fig. 11 3D IR spectra of pyrolytic gases from (a) P0 and (b) P5; 2D IR spectra of pyrolytic gases from (c) P0 and (d) P5.

 © 2025 The Author(s). Published by the Royal Society of Chemistry

Open Access Article. Published on 27 October 2025. Downloaded on 1/19/2026 9:22:09 PM.
This article is licensed under a Creative Commons Attribution-NonCommercial 3.0 Unported Licence.

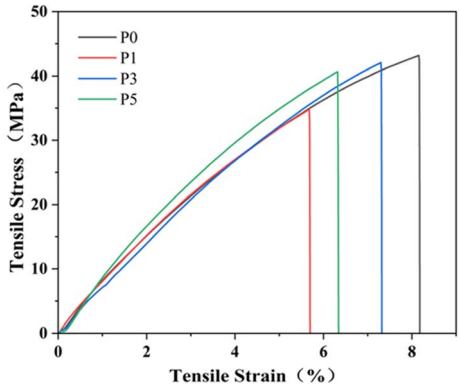

Fig. 12 Tensile stress–train curves of epoxy thermosets doped with PBOZ-DOPO.

exhibited notably lower total gas emission, along with a prolonged release extending up to approximately 800 °C, indicating that PBOZ-DOPO altered the thermal decomposition pathway of the epoxy matrix. In the condensed phase, as previously discussed, phosphorus from PBOZ-DOPO was converted into phosphoric acid, promoting surface charring and thereby inhibiting the decomposition of the underlying epoxy resin. Furthermore, the 2D IR spectra in Fig. 11c and d revealed that the gaseous products from P0 and P5 shared essentially identical compositions: water or aromatic phenols (3652 cm^{-1}), hydrocarbons (2977 cm^{-1}), CO_2 (2360 cm^{-1}), aromatic compounds (1625–1511 cm^{-1}), and ethers (C–O, 1265 and 1176 cm^{-1}), which could be attributed to their similar main molecular structures. Nonetheless, several additional decomposition products were detected in P5, such as carbonyl compounds (1715 cm^{-1}) and nitrogen-containing species like NH_3 (absorption bands between 3800–3600 cm^{-1}). Although the phosphorus content in P5 was only 0.5 wt%, making its direct detection challenging *via* FTIR spectroscopy, phosphorus-containing flame retardants could generate $PO^{\bullet}$ and $PO_2^{\bullet}$ radicals in the gas phase under combustion conditions, as suggested by previous literature.[33] Therefore, in addition to the condensed-phase flame retardant mechanism, a gas-phase flame retardant mechanism was likely operative. Moreover, the abundant nitrogen elements derived from both DDM and PBOZ-DOPO were also expected to act synergistically with phosphorus, further enhancing gas-phase flame retardancy.

Mechanical properties

Tensile tests were conducted to evaluate the mechanical properties of the epoxy thermosets, with the results presented in Fig. 12. The neat epoxy (P0) exhibited characteristic brittle fracture due to its highly cross-linked network. Although the incorporation of the flame retardant generally led to a reduction in both tensile strength and elongation at break for P1, P3, and P5 compared to P0, no distinct trend was observed with increasing loading. This irregularity can be attributed to a balancing effect between two opposing factors: on one hand, the flame retardant could potentially decrease the cross-linking density, thereby weakening mechanical properties; on the other hand, the active OH groups in PBOZ-DOPO participate in the curing reaction with epoxy groups, which helps mitigate the loss of cross-linking density. Furthermore, as shown in Scheme 1, the rigid structure of PBOZ-DOPO, featuring numerous aromatic rings in the main chain and bulky DOPO side groups, could contribute to enhancing the tensile strength. Notably, sample P3 demonstrated a well-balanced retention of mechanical properties, maintaining a tensile strength and an elongation at break reaching 96.4% and 89.4% of P0, respectively.

Conclusions

A polymeric flame retardant, PBOZ-DOPO, featuring active phenolic OH groups, was successfully synthesized *via* the nucleophilic addition of DOPO to a main-chain benzoxazine (PBOZ) and subsequently employed as a co-curing agent and flame retardant for epoxy resin. The resulting epoxy thermosets all maintained good transparency. While TGA and DMA indicated a reduction in thermal stability for the PBOZ-DOPO-modified thermosets (P1–P4), they also displayed increased char yields and a minimal loss in T_g (less than 10 °C), attributable to the macromolecular structure and abundant active phenolic OH groups in PBOZ-DOPO. Moreover, the incorporation of PBOZ-DOPO did not significantly compromise the tensile strength or elongation at break, with P3 showing particularly high retention. The flame retardancy was markedly enhanced, as evidenced by superior UL-94 ratings and higher limiting oxygen index (LOI) values. Specifically, sample P3, with a PBOZ-DOPO content of 4.25 wt% (0.3 wt% phosphorus), achieved a V-0 rating and an LOI of 34.1%. Cone calorimetry tests showed a progressive reduction in the heat release rate, total heat release, and total smoke production from P0 to P5. Further analysis by SEM and Raman spectroscopy confirmed that the amount of graphitized carbon layers formed during combustion increased consistently. Combined with findings from TG-IR analysis, the high flame-retardant efficiency was likely due to a synergistic effect of phosphorus and nitrogen through both condensed-phase and gas-phase flame-retardant mechanisms. Therefore, PBOZ-DOPO reported here was an excellent fire retardant with regard to high transparency, heat resistance and flame retardancy for epoxy resin.

Author contributions

Wei Zhang and Min Liu contributed equally to: conceptualization, investigation, formal analysis, data curation, writing. Honghui Cheng, Jiafeng Di and Geng Huang: data curation. Hua Lai: writing – review & editing.

Conflicts of interest

The authors declare no conflict of interest.

Data availability

All the data for the manuscript is available in the manuscript.

Open Access Article. Published on 27 October 2025. Downloaded on 1/19/2026 9:22:09 PM.
This article is licensed under a Creative Commons Attribution-NonCommercial 3.0 Unported Licence.

Acknowledgements

The authors thank financial support from Hunan Provincial Natural Science Foundation of China (No. 2023JJ50094) and Engineering Technology Center for Advanced Thermal Protection and Flame Retardant Functional Materials (HYNU).

References

1 F.-L. Jin, X. Li and S.-J. Park, *J. Ind. Eng. Chem.*, 2015, **29**, 1–11.
2 M. Rakotomalala, S. Wagner and M. Döring, *Materials*, 2010, **3**, 4300–4327.
3 T. Mariappan and C. A. Wilkie, *Fire Mater.*, 2014, **38**, 588–598.
4 K. A. Salmeia and S. Gaan, *Polym. Degrad. Stab.*, 2015, **113**, 119–134.
5 A. Bifulco, C. Varganici, L. Rosu, F. Mustata, D. Rosu and S. Gaan, *Polym. Degrad. Stab.*, 2022, **200**, 109962.
6 Z. T. Xiao, G. L. Wu, T. M. Yang, Y. Li, Y. Hu, M. Döring and X. Wang, *Chem. Eng. J.*, 2024, **498**, 155484.
7 C. Liu and Q. Yao, *Ind. Eng. Chem. Res.*, 2017, **56**, 8789–8796.
8 W. Peng, S. bin Nie, Y. xuan Xu and W. Yang, *Polym. Degrad. Stab.*, 2021, **193**, 109715.
9 Z. Luo, Y. Lan, J. Cai, Q. Jiang, X. Wang, H. Zhang, L. Hou and L. Xiao, *Eur. Polym. J.*, 2025, **222**, 113605.
10 H. Zhao, H. Duan, J. Zhang, L. Chen, C. Wan, C. Zhang, C. Liu and H. Ma, *Macromol. Mater. Eng.*, 2023, **4**, 22005500.
11 Y. Zhao, Y. Wang, S. Liu, J. Zhao and Y. Yuan, *High Perform. Polym.*, 2016, **29**, 94–103.
12 X. Wang, W. He, L. Long, S. Huang, S. Qin and G. Xu, *J. Therm. Anal. Calorim.*, 2021, **145**, 331–343.
13 Y. Qiu, Z. Liu, L. Qian and J. Hao, *J. Anal. Appl. Pyrolysis*, 2017, **127**, 23–30.
14 H. C. Chang, H. T. Lin and C. H. Lin, *Polym. Chem.*, 2012, **3**, 970.
15 D. Wang, Q. Liu, X. Peng, C. Liu, Z. Li, Z. Li, R. Wang, P. Zheng and H. Zhang, *Polym. Degrad. Stab.*, 2021, **187**, 109544.
16 H. C. Chang, H. T. Lin, C. H. Lin and W. C. Su, *Polym. Degrad. Stab.*, 2013, **98**, 102–108.
17 T. A. Hatsuo Ishida, *Handbook of Benzoxazine Resins*, Elsevier, 2011.
18 C. Shaer, L. Oppenheimer, A. Lin and H. Ishida, *Polymers*, 2021, **13**, 3775.
19 X. Han, R. Chen, M. Yang, C. Sun, K. Wang and Y. Wang, *High Perform. Polym.*, 2022, **34**, 173–183.
20 C. Gérard, G. Fontaine and S. Bourbigot, *Materials*, 2010, **3**, 4476–4499.
21 M. Lounis, S. Leconte, C. Rousselle, L. P. Belzunces, V. Desauziers, J. M. Lopez-Cuesta, J. M. Julien, D. Guenot and D. Bourgeois, *J. Hazard. Mater.*, 2019, **366**, 556–562.
22 R. Jian, P. Wang, W. Duan, J. Wang, X. Zheng and J. Weng, *Ind. Eng. Chem. Res.*, 2016, **55**, 11520–11527.
23 W. Xu, A. Wirasaputra, S. Liu, Y. Yuan and J. Zhao, *Polym. Degrad. Stab.*, 2015, **122**, 44–51.
24 L. Li, S. Li, H. Wang, Z. Zhu, X. Yin and J. Mao, *Polym. Adv. Technol.*, 2021, **32**, 294–303.
25 Y. K. Chen, Q. X. Lu, G. Zhong, H. G. Zhang, M. F. Chen and C. P. Liu, *J. Appl. Polym. Sci.*, 2021, **138**, 1–14.
26 Y. Min, P. Li, X. gang Yin and D. ming Ban, *Polym. Bul.*, 2017, **74**, 1–10.
27 J. W. Yang and Z. Z. Wang, *Phosphorus Sulfur Silicon Relat. Elem.*, 2017, **192**, 1294–1300.
28 P. Wang, F. Yang, L. Li and Z. Cai, *Polym. Degrad. Stab.*, 2016, **129**, 156–167.
29 R. Chen, K. Hu, H. Tang, J. Wang, F. Zhu and H. Zhou, *Polym. Degrad. Stab.*, 2019, **166**, 334–343.
30 Q. Luo, Y. Sun, B. Yu, J. Song, D. Tan, J. Zhao and S. Yan, *Polym. Adv. Technol.*, 2021, **32**, 525–537.
31 C. H. Lin, S. L. Chang, T. Y. Shen, Y. S. Shih, H. T. Lin and C. F. Wang, *Polym. Chem.*, 2012, **3**, 935–945.
32 P. Wang, X. Liu, H. Lai, W. Li, G. Huang, Y. Li and P. Yang, *Polym. J.*, 2022, **54**, 1071–1079.
33 Y. Luo, J. Cai, L. Li, X. Lin, L. Xiao and L. Hou, *Prog. Org. Coat.*, 2023, **184**, 107862.
34 Y. Gou, Y. F. Zha, D. X. Sun, J. H. Yang and Y. Wang, *Polymer*, 2025, **335**, 128827.
35 Z. Huang and Z. Wang, *Polym. Adv. Technol.*, 2021, **32**, 4282–4295.

 © 2025 The Author(s). Published by the Royal Society of Chemistry